London Journal of PHYSICS

Volume 1 No 1

A Shortcut Approximation to the Coupled Equations of Heat and Electric Currents

T. Zhang

Email: zhangtinggang84@gmail.com

August 7, 2024

Abstract

A self-consistent approximation to the coupled equations of heat and electric current densities is developed to facilitate the integration of the relaxation time approximation of the Boltzmann transport equation in a realistic design, analysis, and optimization of energy conversion devices. By introducing two auxiliary energies in the empirical Boltzmann transport equations, the coupled equations can be simply expressed in these auxiliary energies. These auxiliary energies are then determined by optimizing both the heat current through charge neutrality equation without the presence of electric current and the carrier concentrations with the presence of electric current. The heat and the electric current densities as well as the transport properties can then be calculated. The calculated transport properties agreed reasonably well with existing experimental and computational data.

1 Introduction

Most of the existing design, analysis and optimization of thermoelectric devices used temperature-dependent or constant transport properties (1; 2) mostly measured from small samples and the interface and contact effects between their legs and connectors were ignored or accounted for separately. In reality, these transport properties are functions of the electronic band structures that vary with temperature and doping concentration and are affected by the interfacial parameters at the junctions and the contacts. Consequently, the constant or the temperature-dependent transport properties are unable to practically characterize the leg materials of the devices. For realistic device design, analysis, and efficiency and output power projections, more accurate transport properties or direct calculations of the heat and the electric currents of the device are, therefore, necessary. Toward this end, dedicated computational techniques such as the empirical Boltzmann transport equation (3) and the first-principle calculations (4; 5) are available for precise calculation of energy band structure and transport properties. It has been showed in recent reviews (6; 7; 8) that the first-principle calculations can provide accurate equilibrium crystal structure and electronic band structures that can be fed to the Boltzmann transport equation for the calculation of the transport properties with a few or without any empirical parameters. These techniques are developed for the study of the fundamental parameters and the design of advanced materials and are difficult to be employed for device design, analysis and optimization. However, for non-degenerate semiconductors, the relaxation time approximation (RTA) of the Boltzmann transport equation can be used to obtain the coupled equations of heat and electric current densities from which the transport properties can be derived in analytical forms (9) with the energy as a free variable. Since the quantities described by the coupled current equations that are based on the random transport of particles are at macroscopic scale, i.e., heat and electric current densities, the behavior of these quantities must obey the rules/laws for semiconductors at continuum level. From this point of view, this work is aimed to merge the (RTA) Boltzmann transport equation in the device design, analysis, and optimization. A shortcut approximation to the coupled equations of heat and electric current densities is presented. Two auxiliary energies are introduced into the (RTA) Boltzmann transport equation such that the coupled equations of heat and electric current densities can be expressed in these auxiliary energies. These auxiliary energies are then determined by the rules/laws for semiconductors at continuum level with or without the presence of electric current rather than by the first-principle calculations (a shortcut). The heat and the electric current densities as well as the transport properties are then calculated.

 DOI 10.69710/ljp.v1i1.10227

2 Formulations outline

2.1 Governing equations

The relaxation time approximation of the Boltzmann transport equation and the Fermi-Dirac distribution function are used to obtain the coupled equations of heat and electric current densities. By introducing two auxiliary energies, $\Delta E_n = E_F - E_c$ and $\Delta E_p = E_v - E_F$, where E_F is the Fermi level, E_c and E_v are, respectively, the edges of the conduction and the valence bands, the Boltzmann transport equation for electrons and holes in a n-type semiconductor under a given temperature gradient $\nabla_{\mathbf{r}} T$ and an applied field can be expressed as:

$$f_n(E) = f_n^{eq}(E) - \left[\frac{\partial f_n^{eq}(E)}{\partial E}\right] \tau(E)\,\mathbf{v}(E)\cdot\left[\mathbf{F}_n - \nabla_{\mathbf{r}} E_c - \nabla_{\mathbf{r}}(\Delta E_n) - (\eta_n k_B T - \Delta E_n)\left(\frac{\nabla_{\mathbf{r}} T}{T}\right)\right] \tag{2.1}$$

$$f_p(E) = f_p^{eq}(E) - \left[\frac{\partial f_p^{eq}(E)}{\partial E}\right] \tau(E)\,\mathbf{v}(E)\cdot\left[-\mathbf{F}_p - \nabla_{\mathbf{r}} E_v + \nabla_{\mathbf{r}}(\Delta E_p) + (\eta_p k_B T - \Delta E_p)\left[\frac{\nabla_{\mathbf{r}} T}{T}\right]\right] \tag{2.2}$$

where $\mathbf{v}(E)$ is the particle velocity, $\tau(E)$ is the relaxation time, $\mathbf{F}_n$ and $\mathbf{F}_p$ are, respectively, the forces of the field on electrons and holes, $\eta_n = (E - E_c)/(k_B T)$, $\eta_p = (E_v - E)/(k_B T)$, k_B the Boltzmann's constant, T the absolute temperature, and $\mathbf{r}$ the space position (for one-dimensional problem, $\mathbf{r}$ is x).

The electric current density in a semiconductor is defined as:

$$j_n = \int_{E_c}^{\infty} q\,v(E)\,g_n(E)\,[f_n(E) - f_n^{eq}(E)]\,dE \tag{2.3a}$$

where q is electric charge (negative for electron and positive for hole), $g_n(E)$, the density of states of electron, is given by:

$$g_n(E) = \frac{4\pi(2m_n^*)^{3/2}}{h^3}(E - E_c)^{1/2} = g_n^0\,(E - E_c)^{1/2}, \qquad g_n^0 = \frac{4\pi(2m_n^*)^{3/2}}{h^3} \tag{2.3b}$$

in which m_n^* is the effective mass of electron and h is Planck's constant. $v(E)$, the velocity of electron as a function of E, is given by:

$$v^2 = \frac{2}{3m_n^*}(E - E_c) = v_0\,(E - E_c), \qquad v_0 = \frac{2}{3m_n^*}. \tag{2.3c}$$

The energy-dependent relaxation time $\tau(E)$ is given by the power law:

$$\tau(E) = \tau_0\left(\frac{E - E_c}{k_B T}\right)^r \tag{2.3d}$$

where τ_0 is a constant relaxation time and r is the electron scattering parameter.

Introducing Eqs. (2.1), (2.3b), (2.3c) and (2.3d) into the integrand of Eq. (2.3a), the electric current density is obtained as:

$$\begin{aligned} j_n = q\int_0^{\infty} N_0\,e^{\xi_n}\Big\{&[F_n - \nabla_r E_c - \nabla_r(\Delta E_n)]\,(k_B T)^{3/2}\,\eta^{r+3/2}\,e^{-\eta_n} \\ &-\left[(k_B T)^{5/2}\,\eta_n^{r+5/2}\,e^{-\eta_n} - \Delta E_n (k_B T)^{3/2}\,\eta_n^{r+3/2}\,e^{-\eta_n}\right]\left(\frac{\nabla_r T}{T}\right)\Big\}\,d\eta_n. \end{aligned} \tag{2.4a}$$

where $N_0 = \tau_0\,v_0\,g_n^0$ and $\xi_n = (E_F - E_c)/(k_B T)$. Denoting $K_s = \int_0^{\infty} N_0\,(k_B T)^{3/2}\,\eta_n^{s+r+3/2}\,e^{-\eta_n}\,d\eta_n$, Eq. (2.4a) can be re-written in the following compact form:

$$j_n = q e^{\xi_n}\left\{[F_n - \nabla_r E_c - \nabla_r(\Delta E_n)]\,K_0 - (K_1 - K_0\,\Delta E_n)\left(\frac{\nabla_r T}{T}\right)\right\}. \tag{2.4b}$$

The heat current can be defined as:

$$j_q^n = \int_{E_c}^{\infty}(E - E_F)\,v(E)\,g_n(E)\,f_n(E)\,dE \tag{2.5}$$

Introducing Eqs. (2.1), (2.3b), (2.3c), (2.3d) into Eq. (2.5), the heat current is obtained as:

$$j_q^n = -(\Delta E_n)\frac{j_n}{q} + \int_{E_c}^{\infty} \frac{N_n}{k_B T}(E-E_c)^{5/2}\left(\frac{E-E_c}{k_B T}\right)^r e^{(\Delta E_n + E_c - E)/k_B T} \times \left[F_n - \nabla_r E_c - \nabla_r(\Delta E_n) - (\eta_n k_B T - \Delta E_n)\left(\frac{\nabla_r T}{T}\right)\right] dE \tag{2.6a}$$

Re-grouping the terms and using the notation of η_n, ξ_n, and K_s, the heat current can be expressed as:

$$j_q^n = e^{\xi_n}\left\{\left[F_n - \nabla_r E_c - \nabla_r(\Delta E_n)\right] K_1 - (K_2 - K_1 \Delta E_n)\left(\frac{\nabla_r T}{T}\right)\right\} - (\Delta E_n)\frac{j_n}{q} \tag{2.6b}$$

Following the same approach, the coupled equations of heat and electric current densities for holes can also be obtained as below:

$$j_p = -qe^{\xi_p}\left\{K_0\left[-F_p - \nabla_r E_v + \nabla_r(\Delta E_p)\right] + (K_1 - K_0 \Delta E_p)\left(\frac{\nabla_r T}{T}\right)\right\} \tag{2.7}$$

$$j_q^p = e^{\xi_p}\left\{K_1\left[-F_p - \nabla_r E_v + \nabla_r(\Delta E_p)\right] + (K_2 - K_1 \Delta E_p)\left(\frac{\nabla_r T}{T}\right)\right\} + (\Delta E_p)\frac{j_p}{q}. \tag{2.8}$$

where $\xi_p = \Delta E_p/(k_B T)$.

2.2 Self-consistent approximation

Assuming $F_n - \nabla_r E_c \approx 0$, Eqs. (2.4b) and (2.6b) can be approximated by:

$$j_n = qe^{\xi_n}\left[-K_0 \nabla_r(\Delta E_n) - (K_1 - K_0 \Delta E_n)\left(\frac{\nabla_r T}{T}\right)\right] \tag{2.9a}$$

$$j_q^n = e^{\xi_n}\left[-K_1 \nabla_r(\Delta E_n) - (K_2 - K_1 \Delta E_n)\left(\frac{\nabla_r T}{T}\right)\right] - (\Delta E_n)\frac{j_n}{q} \tag{2.9b}$$

The transport properties, Seebeck coefficient (α), electrical conductivity (σ), and electronic thermal conductivity (κ), can be derived from Eq. (2.9) and are expressed, respectively, as:

$$\alpha_n = \frac{1}{qT}\left(\Delta E_n - \frac{K_1}{K_0}\right) = \frac{k_B}{q}\left[\xi_n - \left(r + \frac{5}{2}\right)\right] \tag{2.10a}$$

$$\sigma_n = \frac{q^2}{T} K_0 = q^2\left(\frac{8\tau_0}{3 m_n^* \sqrt{\pi}}\right)\left(\frac{2\pi m_n^* k_B T}{h^3}\right)^{3/2} e^{\Delta E_n/k_B T}\Gamma(r + 5/2) \tag{2.10b}$$

$$\kappa_n = \frac{1}{T^2}\left(K_2 - \frac{K_i^2}{K_0}\right) = \frac{e^{\Delta E_n/k_B T}}{T}\left(\frac{4\tau_0 (k_B T)^2}{3 m_n^* \sqrt{\pi}}\right)\left(\frac{2\pi m_n^* k_B T}{h^3}\right)^{3/2}\Gamma(r + 7/2) \tag{2.10c}$$

Similarly, Eqs. (2.7) and (2.8) can be approximated by:

$$j_p = -qe^{\xi_p}\left\{K_0 \nabla_r(\Delta E_p) + (K_1 - K_0 \Delta E_p)\left(\frac{\nabla_r T}{T}\right)\right\} \tag{2.11}$$

$$j_q^p = e^{\xi_p}\left\{K_1 \nabla_r(\Delta E_p) + (K_2 - K_1 \Delta E_p)\left(\frac{\nabla_r T}{T}\right)\right\} + (\Delta E_p)\frac{j_p}{q}. \tag{2.12}$$

The transport properties for holes can also be obtained from Eqs. (2.11) and (2.12) as:

$$\alpha_p = \frac{1}{qT}\left(\Delta E_p - \frac{K_1}{K_0}\right) = \frac{k_B}{q}\left[\left(r + \frac{5}{2}\right) - \xi_p\right] \tag{2.13a}$$

 DOI 10.69710/ljp.v1i1.10227

$$\sigma_p = \frac{q^2}{T} K_0 = q^2 \left(\frac{8\tau_0}{3 m_p^* \sqrt{\pi}} \right) \left(\frac{2\pi m_p^* k_B T}{h^3} \right)^{3/2} e^{\Delta E_p / k_B T} \Gamma(r+5/2) \tag{2.13b}$$

$$\kappa_p = \frac{1}{T^2} \left(K_2 - \frac{K_i^2}{K_0} \right) = \frac{e^{\Delta E_p / k_B T}}{T} \left(\frac{4\tau_0 \, (k_B T)^2}{3 m_p^* \sqrt{\pi}} \right) \left(\frac{2\pi m_p^* k_B T}{h^3} \right)^{3/2} \Gamma(r+7/2) \tag{2.13c}$$

where m_p^* is the effecive mass of hole.

The bipolar transport properties are then calculated by the following equations:

$$\alpha = \frac{\alpha_n \sigma_n + \alpha_p \sigma_p}{\sigma} \tag{2.14a}$$

where σ is given by:

$$\sigma = \sigma_n + \sigma_p \tag{2.14b}$$

$$\kappa = \kappa_n + \kappa_p + \frac{\sigma_n \sigma_p}{\sigma} \left(\alpha_p - \alpha_n \right)^2 T. \tag{2.14c}$$

The auxiliary energies, ΔE_n and ΔE_p, are determined at macroscopic level using the rules/laws for semiconductors with and without the presence of electric current ($j = 0$ and $j \neq 0$).

For $j = 0$, $\nabla_r T / T$ is firstly solved from Eq. (2.9a) and is then introduced into Eq. (2.9b) to solve for $\nabla_r(\Delta E_n)$ which is given by:

$$\nabla_r(\Delta E_n^0) = j_q^{n0} e^{-\xi_n^0} \frac{K_1 - K_0 \Delta E_n^0}{K_0 K_2 - K_1^2} \tag{2.15}$$

in which the superscript 0 denotes the variables obtained at $j = 0$. Similarly, for holes, $\nabla_r(\Delta E_p)$ is given by:

$$\nabla_r(\Delta E_p^0) = j_q^{p0} e^{-\xi_p^0} \frac{K_1 - K_0 \Delta E_p^0}{K_1^2 - K_0 K_2}. \tag{2.16}$$

It is assumed that j_q^{n0} and j_q^{p0} can be calculated, respectively, by:

$$j_q^{n0} = -k_q^n \frac{dT}{dx} \tag{2.17a}$$

and

$$j_q^{p0} = -k_q^p \frac{dT}{dx} \tag{2.17b}$$

where k_q^n and k_q^p are considered as the mean thermal conductivity. At $j = 0$, the charge neutrality condition should be observed, i.e., $N_D - N_A + p - n = 0$, where N_D and N_A are the donor and acceptor concentration, p and n are the carrier concentration for electron and hole, respectively. k_q^n and k_q^p are determined, respectively, by Eq. (2.10c) and (2.13c) iteratively and simultaneously using ΔE_n and ΔE_p determined by the neutrality condition until they are converged to constants (within the allowed errors). The respective auxiliary energies are then considered as ΔE_n^0 and ΔE_p^0. The current densities calculated by (2.17) are the heat current densities without the presence of electric current ($j = 0$).

For $j \neq 0$, $\nabla_r T / T$ is firstly solved from Eq. (2.9b) and is then introduced into Eq. (2.9a) along with Eq. (2.15) to obtain the electric current density as given below:

$$j_n = \frac{q \left[j_q^{n0} \left(K_1 - K_0 \Delta E_n^0 \right) e^{\xi_n - \xi_n^0} - j_q^n \left(K_1 - K_0 \Delta E_n \right) \right]}{\Delta E_n (K_1 - K_0 \Delta E_n) - (K_2 - K_1 \Delta E_n)} \tag{2.18a}$$

Using Eq. (2.15) and $\nabla_r T / T$ for $j = 0$, heat current density can also be approximated by:

$$j_q^n = j_q^{n0} e^{\xi_n - \xi_n^0} \left[\frac{\left(\Delta E_n^0 - \Delta E_n \right) \left(K_1 - K_0 \Delta E_n \right) K_0}{K_0 K_2 - K_1^2} + \frac{j_q^n}{j_q^{n0}} \right] \tag{2.18b}$$

 DOI 10.69710/ljp.v1i1.10227

Similarly, the heat and electric current densities for the minority carriers (holes) can also be obtained:

$$j_p = \frac{q\left[j_q^p\,(K_0\,\Delta E_p - K_1) + j_q^{p0}\,\left(K_1 - K_0\,\Delta E_p^0\right)\,e^{\xi_p - \xi_p^0}\right]}{(K_2 - K_1\Delta E_p) - \Delta E_p(K_1 - K_0\,\Delta E_p)} \tag{2.19a}$$

and

$$j_q^p = j_q^{p0}\,e^{\xi_p - \xi_p^0}\left[\frac{\left(\Delta E_p - \Delta E_p^0\right)\,(K_1 - K_0\,\Delta E_p)\,K_0}{K_1^2 - K_0\,K_2} + \frac{j_q^p}{j_q^{p0}}\right]. \tag{2.19b}$$

At $j \neq 0$, the energy band structure and the carrier concentrations should be different from those at $j = 0$. Since the carrier distribution is time-independent, the system is in steady state. A steady system should stay at a stable state. Based on this scenario, the auxiliary energies at $j \neq 0$, ΔE_n and ΔE_p, are determined by finding the stationary points of the carrier concentrations, i.e.,:

$$\left.\frac{d\,n}{d(\Delta E_n)}\right|_T = \frac{d}{d(\Delta E_n)}\int_{E_c}^{\infty} g_n(E)\,[f_n(E) - f_n^{eq}(E)]\,dE = 0 \tag{2.20a}$$

and

$$\left.\frac{d\,p}{d(\Delta E_p)}\right|_T = \frac{d}{d(\Delta E_p)}\int_{-\infty}^{E_v} g_p(E)\,\left[f_p(E) - f_p^{eq}(E)\right]\,dE = 0. \tag{2.20b}$$

The auxiliary energies obtained from Eqs. (2.20) are used to calculate the heat and electric current densities using Eqs. (2.18) and (2.19), respectively.

3 Results and discussion

Formulations outlined in section 2 were used to determine the heat and the electric current densities of a n-type Silicon semiconductor. The semiconductor has an effective mass of $m_n^* = 0.36m_e$ for electron and of $m_p^* = 0.81m_e$ for hole, where m_e is the mass of free electron. The temperature gradient used in the calculations is $dT/dx = 1.0{\cdot}10^5$ K/m. Changes of the auxiliary energies, ΔE_n and ΔE_p, with temperature are firstly presented for different doping concentrations. The transport properties are then given. Subsequently, the heat and the electric current densities are presented for different temperature and doping concentrations.

3.1 Auxiliary energies – ΔE_n and ΔE_p

The auxiliary energies at $j = 0$, ΔE_n^0 and ΔE_p^0, and at $j \neq 0$, ΔE_n and ΔE_p, were calculated for different donor concentrations (N_D) and temperatures. These results are shown in Fig. 1. For $j = 0$, these results (Fig. 1a) are basically the same as those calculated using the following equations given in (10; 11):

$$n_n = \frac{1}{2}\left[N_D - N_A + \sqrt{(N_D - N_A)^2 + 4n_i^2}\right] \qquad n_p = \frac{n_i^2}{n_n} \tag{3.1a}$$

$$E_{Fn} - E_c = k_B\,T\,\ln\left(\frac{n_n}{N_c}\right) \qquad E_v - E_{Fn} = k_B\,T\,\ln\left(\frac{p_n}{N_v}\right) \tag{3.1b}$$

where n_n and p_n are, respectively, the electron and hole concentrations of the n-type semiconductor, N_c and N_v are the effective densities of state of the conduction and the valence bands, respectively, E_{Fn} is the Fermi level, and n_i is the intrinsic carrier concentration calculated by:

$$n_i = \sqrt{N_c N_v}\,e^{-E_g/(2k_B T)}. \tag{3.1c}$$

Considering that ΔE_n^0 and ΔE_p^0 are obtained at $j = 0$ and that Eq. (3.1) are obtained at thermal equilibrium condition without any external excitation (not shown), the agreement between these two results can be justified.

For $j \neq 0$, ΔE_n and ΔE_p are shown in Fig. 1b. Comparison between Fig. 1a and 1b shows that ΔE_n and ΔE_p are lower than ΔE_n^0 and ΔE_p^0. Their slopes are also different. These differences can be understood that as electric current flows through the semiconductor, its energy level changes and becomes lower than those at $j = 0$.

From Fig. 1, it can be observed that $|\Delta E_n| < |\Delta E_p|$, which indicates that the Fermi level, E_{Fn}, is close to the conduction band edge, a common characteristics for n-type semiconductors.

 DOI 10.69710/ljp.v1i1.10227

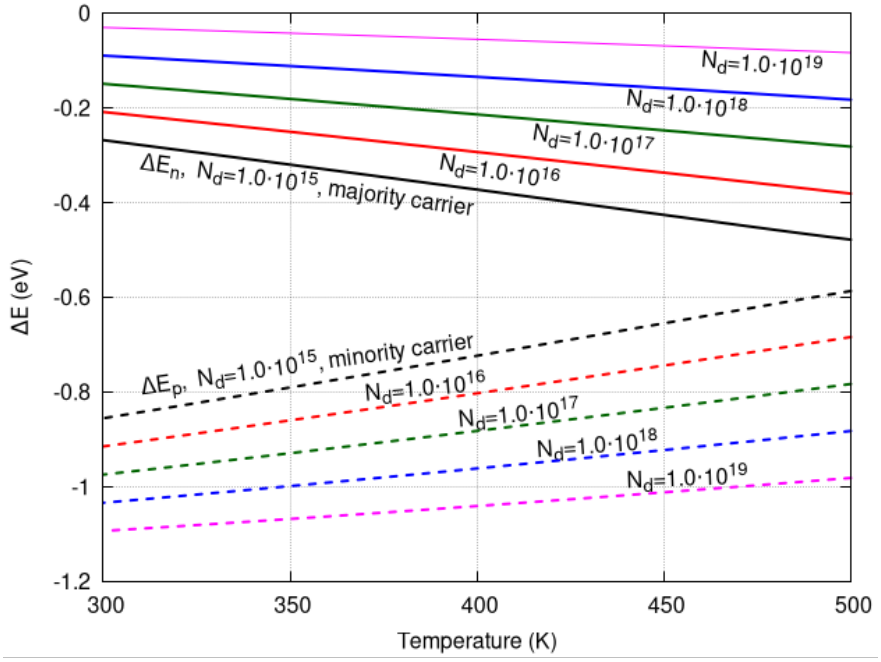

(a)

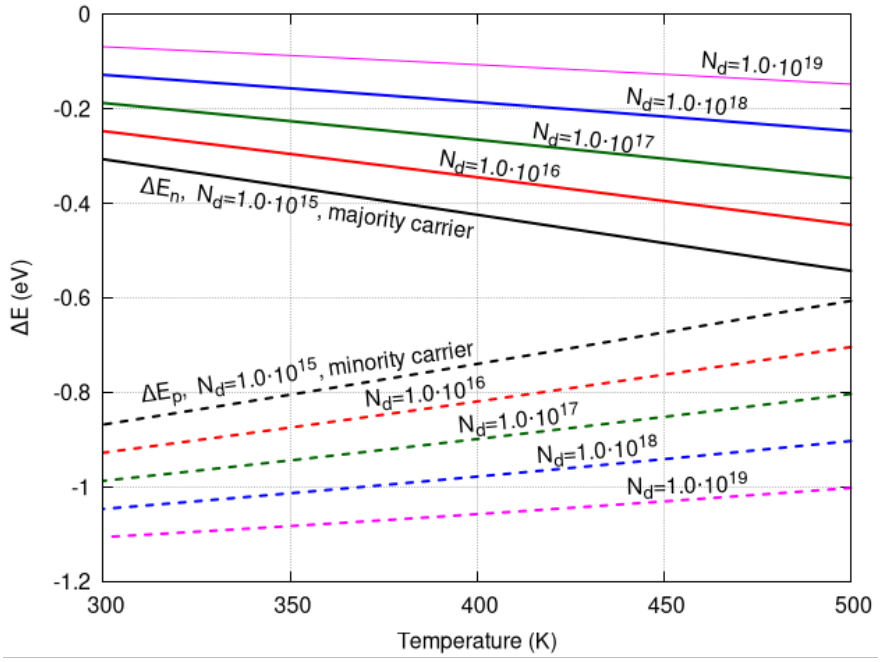

(b)

Figure 1: Variation of (a) ΔE_n^0 and ΔE_p^0 and (b) ΔE_n and ΔE_p with temperature and doping concentratioin.

 DOI 10.69710/ljp.v1i1.10227

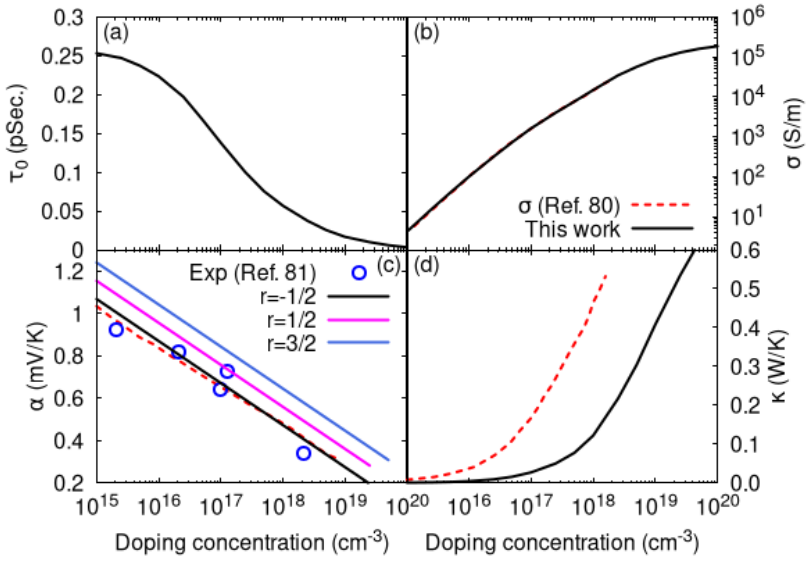

Figure 2: Thermoelectric transport properties vary with doping concentration. (a) Constant relaxation time, τ_0, used in current work to calculate the transport properties. (b) Electrical conductivity, σ. (c) Seebeck coefficient, α. (d) Electronic thermal conductivity, κ. Dashed lines are for (12). Solid lines are for the current work. Open circle is for experimental data (13).

3.2 Transport properties

The transport properties calculated from Eqs. (2.10a), (2.10b), and (2.10c) are shown in Fig. 2. Equations (2.10b) and (2.10c) indicate that σ, and κ are directly affected by the scattering parameters τ_0 and r. For a fixed r, the constant relaxation time τ_0 needs to be adjusted such that either σ or κ can be better correlated with existing data. These two parameters, τ_0 and r, are the only parameters needed to be adjusted in this self-consistent approximation. τ_0 used in the current calculations to correlate with the existing data for σ is shown in Fig. 2a for $r = -1/2$. As it can be observed from Fig. 2b that the agreement between the current calculation and the existing calculation data (12) for σ at 300 K is very well. However, the correlation for κ is not as good as that for the σ as shown in Fig. 2d. The ratio between the κ and the σT, $\kappa/\sigma T$, calculated in the current work for the considered doping densities is $6.65608{\cdot}10^{-8}$W-Ω/K^2 higher than the Lorentz number for metals, $2.4453{\cdot}10^{-8}$W-Ω/K^2. Figure 2c shows the computed results for α. Since α is independent of τ_0 and the scattering parameter r can be a constant for different doping concentrations, three rs were used for the calculations, i.e., $-1/2$, $1/2$, and $3/2$. The results show that $r = -1/2$ gives better correlation with the experimental data (13) and the existing simulation data.

3.3 Electric current density

Figure 3 shows the changes of electric current density with temperature and doping concentrations. The electric current density decreases with temperature and increases with doping concentration. As Eqs. 2.3a and 2.18a indicate that the electric current density is a function of electron potential, energy band gap, density of states, and heat current. Both electron potential and band gap decrease with temperature as shown in Fig. 1. In these results, the decrease of electric current with temperature is mainly caused by the decrease of heat current as to be discussed in the subsequent section. Electric current increases with doping concentration can be easily understood. As the numbers of the charge carriers increases, electric current increases accordingly. However, as the number of charge carriers increases, electron scattering also increases. As a result, the increases of the electric current with doping concentration is reduced as shown in the these figures. This is consistent with the electrical conductivity as shown in Fig. 2b.

3.4 Heat currents

Heat current densities with and without the presence of electric current in the semiconductor were calculated for the given temperature gradient. Figure 4a shows the heat currents without the presence of electric current while Fig. 4b

 DOI 10.69710/ljp.v1i1.10227

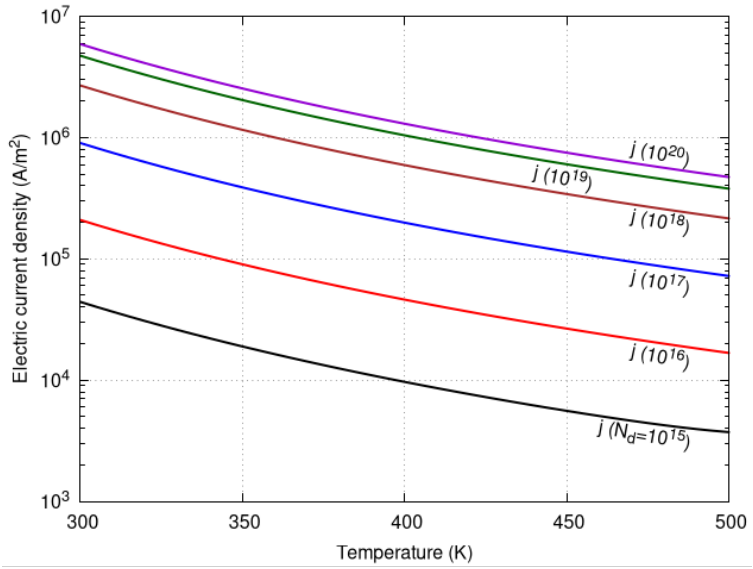

(a)

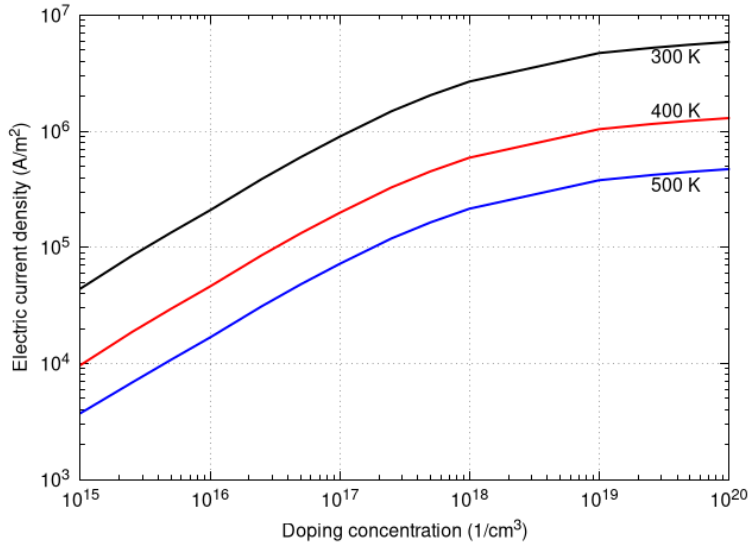

(b)

Figure 3: Electric current densities vary with temperature and doping concentrations. (a) Electric current density vary with temperature for the given doping concentrations. (b) Electric current density vary with doping concentration for the given temperature.

 DOI 10.69710/ljp.v1i1.10227

shows those with the presence of electric current. Similar to the electric current densities, these heat currents depend on electron potential, energy band gap, density of states, and electric current. These results showed that the heat currents with or without the presence of electric current decreased with temperature. This is consistent with the thermal conductivity which decreases with temperature. These figures also showed that the heat currents increased with the doping concentration which is also consistent with the thermal conductivity that increases with doping concentration. The increase of the heat current with doping concentration is nonlinear. At lower doping concentration, the increase is large. As the doping concentration increases, the increase gradually becomes smaller. These results also showed that the heat current with the presence of electric current was larger than that without the electric current for a given doping concentration and a temperature. The difference between j_q^{n0} and j_q^n is large at lower doping concentration. As the doping concentration increases, their difference decreases and eventually they become nearly the same at about $N_D = 2.5 \cdot 10^{19}$ cm^{-3}. This result can also be deduced from Eq. (2.18b) which shows that the heat current with the presence of electric current is calculated by j_q^{n0} scaled by a factor of function of the ΔE_n^0 and ΔE_n. As ΔE_n^0 and ΔE_n becomes close to each other at higher doping concentration, the factor becomes close to 1.0. As a result, $j_q^n \approx j_q^{n0}$. These results explained the heating effect of electric current in a semiconductor.

The proposed self-consistent approximation to the coupled transport equations of heat and electric current densities can provide good characterizations of the transport properties and the heat and the electric current densities. By introducing the auxiliary energies, ΔE_n and ΔE_p into the (RTA) Boltzmann transport equation, and using the generic equations for the effective density of states, the carrier velocity derived directly from the kinetic energy, and the power law for the energy-dependent relaxation time, the coupled equations of heat and electric current densities can be expressed in these auxiliary energies. Considering that at zero electric current, the system should be neutral and the charge carriers should be balanced, these auxiliary energies are determined by optimizing the heat current using charge neutrality conditions. Considering that the (RTA) Boltzmann transport equation is time-independent thus the particle distribution is in steady state and that a steady system should be stable, for non-zero electric current, the auxiliary energies are determined by finding the stationary points of the carrier concentrations. By such a self-consistent approximation, the needs for the calculation or adjustment of the chemical potentials are not necessary. Consequently, the (RTA) Boltzmann transport equation can be easily merged in the device design, analysis, and optimization to determine the transport properties realistically. The calculated Seebeck coefficient agreed very well with experimental and existing computational data using $r = -1/2$. By adjusting the constant relaxation time, τ_0, for different doping concentrations, the electrical conductivity also agreed very well with the existing computational data. By comparing the calculated ratio of the electronic thermal conductivity to the electrical conductivity multiplied by temperature, $\kappa/\sigma T$, with the Lorentz number, the electronic thermal conductivity was found to be overestimated in the current work. The heat and the electric current densities can also be calculated in the current approximation. From these current densities, the output power and the efficiency of the device can be directly evaluated without resorting to the transport properties. These will be invaluable information for the deign, analysis, and optimization of semiconductor devices.

In this proposed approximation, the power law of the energy-dependent relaxation time plays a considerable role in the calculation of the transport properties, the heat and the electric current densities. And, its constant relaxation time, τ_0, and power, r, are the only parameters needed to be adjusted for better correlation with experimental data. More accurate formulation for relaxation time or electron/phonon scattering is needed for realistic design, analysis, and optimization of semiconductor devices.

4 Conclusions

Thermoelectric transport properties vary as the legs are integrated into the devices, thus temperature-dependent or constant properties used in the design, analysis, and optimization of these devices cannot accurately characterize the leg materials. The proposed self-consistent approximation can easily merge the (RTA) Boltzmann transport equation in the design, analysis, and optimization of thermoelectric devices for realistic characterization of the transport properties of the materials without resorting to high-level computation such as the first principle calculation. This approximation can also calculate the heat current density with and without the presence of electric current and the electric current density, which are invaluable information for direct determination of the efficiency and the output power of the devices without resorting to the transport properties. Development of more accurate formulation for the relaxation time or electron/phonon scattering could minimizing or remove the need for correlation with experimental data.

 DOI 10.69710/ljp.v1i1.10227

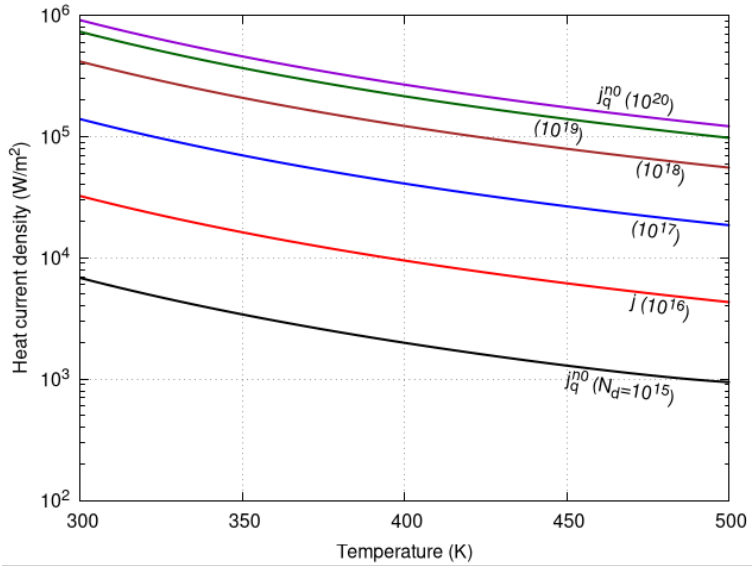

(a)

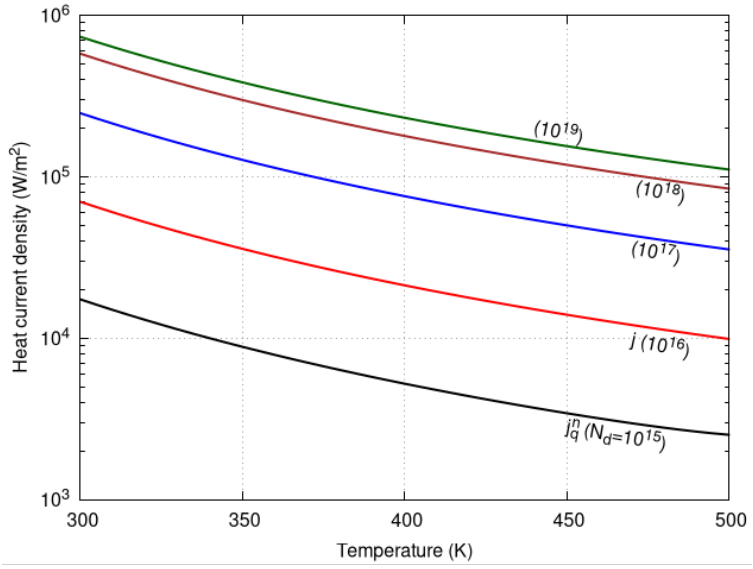

(b)

Figure 4: Heat current density vary with temperature and doping concentration. (a) Heat current density without the presence of electric current. (b) Heat current density with the presence of electric current.

 DOI 10.69710/ljp.v1i1.10227

5 Copyright Notice

References

[1] T. Zhang, New thinking on modeling of thermoelectric devices, Applied Energy 168 (2016) 65–74.

[2] T. Zhang, Integrating material engineering with module design optimization: A new design concept for thermoelectric generator, Energy 148 (2018) 397–406.

[3] M. Ziman, Electrons and Phonons: The Theory of Transport Phenomena in Solids, Oxford University Press,USA, 2001.

[4] P. Hohenberg, W. Kohn, Inhomogeneous electron gas, Phys. Rev. 136 (1964) B864–71.

[5] W. Kohn, L. J. Sham, Self-consistent equations including exchange and correlation effects, Phys. Rev. 140 (1965) A1133–8.

[6] J. Zhou, B. Liao, G. Chen, First-principles calculations of thermal, electrical, and thermoelectric transport properties of semiconductors, Semiconductor Science and Technology 31 (2016) 043001. doi:10.1088/0268-1242/31/4/043001.

[7] J. J. G. Moreno, J. Cao, M. Fronzi, M. H. N. Assadi, A review of recent progress in thermoelectric materials through computational methods, Materials for Renewable and Sustainable Energy 9 (2020) 16. doi:10.1007/s40243-020-00175-5.

[8] A. S. Chaves, M. Pizzochero, D. T. Larson, A. Antonelli, E. Kaxiras, Semiclassical electron and phonon transport from first principles: Application to layered thermoelectrics, Journal of Computational Electronics 22 (2023) 1281–1309.

[9] G. S. Nolas, H. J. Goldsmid, Thermal conductivity of semiconductor, in: T. M. Tritt (Ed.), Thermal Conductivity: Theory, Propeeties, and Applications, Kluwer Academic/Plenum Publishers, 2004, pp. 105–121.

[10] A. S. Grove, Physics and Technology of Semiconductor Devices, Wiley, New York, 1967.

[11] S. Sze, Semiconductor devices, physics and technology, 2nd Ed., New York, NY: John Wiley and Sons, 2002.

[12] Z. Wang, S. D. Wang, S. Obukhov, N. Vast, J. Sjakste, V. Tyuterev, N. Mingo, Thermoelectric transport properties of silicon: Toward an ab initio approach, Phys Rev B 83 (2011) 205208.

[13] T. H. Geballe, G. W. Hull, Seebeck effect in silicon, Phys Rev 98 (1955) 940.

List of Figures